Journal of Industrial Microbiology & Biotechnology (2020) 47:725–738
https://doi.org/10.1007/s10295-020-02293-5

SIMB
Society for Industrial Microbiology and Biotechnology

FERMENTATION, CELL CULTURE AND BIOENGINEERING - MINI REVIEW

Biophysical methods to quantify bacterial behaviors at oil–water interfaces

Jacinta C. Conrad[1]

Received: 31 May 2020 / Accepted: 16 July 2020 / Published online: 2 August 2020

Abstract

Motivated by the need for improved understanding of physical processes involved in bacterial biodegradation of catastrophic oil spills, we review biophysical methods to probe bacterial motility and adhesion at oil–water interfaces. This review summarizes methods that probe bulk, average behaviors as well as local, microscopic behaviors, and highlights opportunities for future work to bridge the gap between biodegradation and biophysics.

Keywords Adhesion · Motility · Accumulation · Oil–water Interface

Introduction

Interactions of bacteria with a nearby interface play a crucial role in their ecology, including biofilm formation [1]. Whereas the vast majority of studies of bacteria at interfaces have focused on solid surfaces, bacterial interactions with fluid–fluid interfaces remain understudied despite their environmental and technological importance. For example, adhesion of bacteria to hydrocarbon–water interfaces plays a role in the reaction kinetics in a two-phase bioreactor [2] and in the motion of droplets driven by bacterial motility [3, 4]. Air–liquid or liquid–liquid interfaces are often decorated with surfactants to control the interfacial stability, and thus, there is particular interest in understanding how surfactants affect bacterial behaviors at surfactant-laden interfaces. This understanding offers, as one example, new opportunities to engineer biomaterials: addition of surfactant to a suspension of cellulose-producing bacteria led to the formation of a macroporous foam of bacterial cellulose [5].

A recent and striking example of bacterial interactions with the interface between two liquids arose in the context of biodegradation, one of the most important remediation strategies for underwater oil spills [6]. After the catastrophic Deepwater Horizon MC252 (DWH) well blowout in 2010, hydrocarbon-degrading microorganisms increased in numbers in the Gulf of Mexico [7, 8] and in nearby coastal environments [9], suggesting that metabolism of oil and natural gas by microbes played a role in the unexpectedly rapid disappearance [10, 11] of the 780,000 m^3 of light crude oil [12] released into the Gulf. Community studies revealed that the indigenous bacterial populations were enriched in genera such as *Alcanivorax*, *Marinobacter*, and *Rhodobacteraceae* that were thought to play a role in the rapid oil degradation [9]. Approximately, half of the hydrocarbons were released as gases and were rapidly consumed during the early months of the spill [8, 10]; thus, emergency response strategies focused on remediation of the liquid oil.

As part of the emergency response, chemical dispersants were applied at the surface and injected at the wellhead to break oil into smaller droplets [13, 14] and thereby increase the surface area per volume to speed degradation and weathering [15]. Approximately, 0.68 million gallons of two commercial dispersants (Corexit 9500 and 9527) were applied at the wellhead with a targeted dispersant:oil ratio of 1:25 [16, 17]. Although the dispersant is proprietary and its exact composition not publicly available, Corexit contains approximately 10% dioctyl sodium sulfosuccinate (DOSS), a small-molecule surfactant that is thought to facilitate rapid adhesion of dispersants to the oil–water interface [18]. During DWH, addition of Corexit led to a decrease in the mean droplet diameter, from ~ 200 µm (with no dispersant, characteristic of the size scale of turbulent eddies in the ocean [19]) to ~ 10 µm (with dispersant) [20]. Although large droplets rose to the ocean surface and were skimmed or burned, droplets of diameter 10–60 µm were

✉ Jacinta C. Conrad
jcconrad@uh.edu

[1] Department of Chemical and Biomolecular Engineering, University of Houston, Houston, USA

neutrally buoyant in the Gulf waters and were transported as a disperse cloud [21] that was generally more accessible to microbes. Larger, buoyant droplets of diameter ~300 µm rose to the surface and formed a thin slick there [22].

Overall, the National Incident Command's Flow Rate Technical Group estimated that the fate of approximately 50% of the oil released from DWH (8% chemically dispersed, 17% naturally dispersed, and 25% residual oil [23]) was determined by degradation by bacteria [11]. Thus, understanding the effects of biodegradation coupled to those of surfactant addition is necessary to accurately predict dispersal of spilled oil [24]. This understanding, however, is complicated by the competing effects of bacterial processes along with physicochemical processes that affect spilled oil. For example, bacteria can naturally produce surfactants [25, 26] and extracellular polymeric substances (EPS) that can emulsify oil to form droplets in seawater, although less effectively than the commercial dispersant Corexit [27]. In turn, the EPS produced by adherent bacteria can modify droplet transport in the water column by increasing the viscous drag on a rising droplet [28, 29]. As a final example, simulations suggest that motile, chemotactic bacteria consume rising, buoyant droplets of hydrocarbons faster than nonmotile bacteria, but that the advantage imparted by chemotaxis decreases as the droplet diameter is increased [30].

The complex nature of the prolonged DWH oil spill precludes a simple answer as to whether subsurface application of dispersants enhanced biodegradation in the Gulf of Mexico [14]. Nonetheless, this question remains of intense interest for oil-spill response. Studies, however, report contrasting effects of dispersants on bacterial growth and biodegradation. Microcosm experiments replicating surface and deepwater conditions in the Gulf of Mexico suggested that addition of Corexit enriched dispersant-consuming species (e.g., *Colwellia*) at the expense of hydrocarbon-degrading species (e.g., *Marinobacter*), reducing the overall rate of biodegradation [31]. These changes occurred as part of the broader evolution of microbial community structure after DWH, as revealed through mesocosm experiments suggesting that rare taxa increased in abundance after DWH [32]. Likewise, in a microbial community deposited on a Louisiana beach, Corexit reduced the viability of hydrocarbon-degrading *Marinobacter*; whereas, non-degrading *Vibrio* bacteria increase in abundance [33]. By contrast, experiments using surface seawater from the northeastern Gulf also find a shift in community composition but instead suggest that dispersant addition enhances the biodegradation rate [34]. Similarly, deepwater samples from the Gulf of Mexico acquired after DWH suggest that addition of Corexit enhanced biodegradation and lead to enrichment of *Colwellia* and *Oceanospirillales* species [35]. Experiments showing enhancement in degradation upon surfactant addition are consistent with studies from other environments, including off eastern Canada [36] and Halifax Harbor [37]. Microcosm studies also report contrasting effects of dispersants on the composition and metabolic activity of bacteria in consortia [38].

Finally, dispersant use affects other processes beyond bacterial growth and biodegradation. In the DWH spill, up to 14% of the oil released into the environment accumulated in marine oil snow (MOS) [39], agglomerates of bacteria, organic matter, and hydrocarbons that are more dense than water [40]. MOS was intensely studied after DWH because its sedimentation may have facilitated rapid transport of the spilled oil to the Gulf floor [41]. Whereas addition of oil appeared to enhance MOS formation [42, 43], contrasting effects were reported upon addition of Corexit. The dispersant enhanced MOS formation for bacteria [44] but not for diatoms [43]. This example suggests that dispersant effects on bacterial interactions with hydrocarbons can alter other mechanisms responsible for the transport and fate of spilled oil in marine environments.

Collectively, these studies suggest that the rate of degradation by bacteria depends in part on their interactions, physicochemical as well as biological, with dispersed hydrocarbons. The practical need to understand how dispersants affect these interactions and hence degradation [14] has, in recent years, motivated physical studies of bacterial behaviors at the oil–water interface. How macro-scale observations of degradation of hydrocarbons by bacteria connect to micro-scale bacterial behaviors at the interface, however, remains incompletely understood. As one example, lab-scale experiments examining a variety of surfactants, including DOSS and Corexit EEC9500A, on growth of *Alcanivorax borkumensis*, a marine oil-degrading bacterium, found that only nonionic Tween 20 increases the growth of bacteria [45]. Microscopic examination of oil droplets revealed that suspensions of *A. borkumensis* form oil-in-water emulsions (Fig. 1a), attributed to biosurfactant production and to attachment of bacteria at the oil–water interface. Bacteria grown for longer times in the presence of hexadecane attach more readily to a hexadecane–water interface, as indicated by a decrease in the interfacial tension over time [46] (Fig. 1b). Addition of Corexit EEC9500A reduces the attachment of *A. borkumensis* bacteria on the oil–water interface, and addition of Tween 20 eliminates it entirely, although these bacteria in the water phase are able to metabolize Tween 20 [47]. Formation of mature *A. borkumensis* biofilms at the oil–water interface, however, reduces the effectiveness of Corexit at dispersing oil [48]. Thus, lab-scale physical observations can complement and extend understanding of degradation processes occurring in natural, complex systems.

In this mini-review, we survey methods for physical studies of bacteria at oil–water interfaces and highlight insights into bacterial behaviors obtained from these

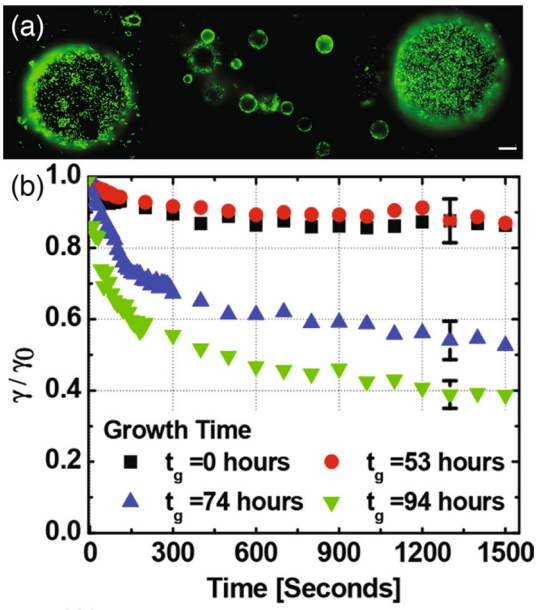

Fig. 1 Physical studies of the oil-degrading bacterium *Alcanivorax borkumensis*. **a** Fluorescence micrograph of *A. borkumensis* attached to hexadecane in artificial sea water. Reprinted with permission from Ref. [47]. Copyright (2018) American Chemical Society. **b** Normalized interfacial tension γ/γ_0 for suspensions of *A. borkumensis* grown for the indicated times in the presence of hexadecane. Reprinted with permission from Ref. [46]. Copyright (2018) American Chemical Society

studies. This focus on biophysical methods complements recent reviews on microbial biodegradation [49, 50] and on cell surface hydrophobicity [51]. We describe ensemble and bulk methods, summarize recent studies that apply single-cell experiments and simulations to characterize heterogeneity and interactions, and list avenues for further research.

Bulk methods

Quantitatively interrogating the response of bacteria at liquid–liquid interfaces is challenging. Many methods for probing bacterial interfaces with surfaces involve solid substrates. These methods include quartz crystal microbalance with dissipation (QCM-D, reviewed for bacteria in Ref. [52]) and atomic force microscopy (AFM, reviewed for bacteria in Ref. [53]). By contrast, fewer methods directly probe interactions of bacteria at the interface between two liquids. Here, we summarize bulk methods that directly assess the interactions of bacteria with dispersed hydrocarbons, focusing on those that permit or enable studies at the liquid–liquid interface.

Hydrophobicity

Bacterial surface hydrophobicity can be quantified through the contact angle of water, typically measured on a lawn of bacteria grown on a flat, solid substrate. As one example, contact angle measurements revealed that *Mycobacterium frederiksbergense* grown on mixtures of hydrophobic anthracene and hydrophilic glucose increase in hydrophobicity with increasing anthracene fraction (from 34° to 54–63°) [54]. Contact angle measurements of several liquids on the lawn enable the calculation of the surface energy, through the methods of Wu [55] or Owens, Wendt, Rabel, and Kaelble (OWRK) [56–58]. Determination of the surface energy is useful for understanding interactions with liquid oil because thermodynamics plays a central role in determining the affinity of bacteria for a surface [59]. Bacteria of low surface energy are likely to interact more readily with dispersed hydrocarbons, whose surface energies are generally lower than that of water.

The microbial adhesion to hydrocarbons (MATH) assay [61] is one of the most widely used methods to probe the affinity of bacteria for dispersed hydrocarbons. In this assay, the turbidity of an aqueous phase containing bacteria is measured before and after vortex mixing with a liquid hydrocarbon. Cells that adhere to the hydrocarbon droplets are removed from the aqueous phase into an emulsion, which creams. Thus, the decrease in adsorbance of the aqueous phase after mixing reflects the extent to which cells are captured by the hydrocarbon phase [62]. Assay results are reported as a percentage of the initial absorbance, reflecting the percentage of cells that remain in the hydrophilic phase, or as the percentage adhering to the hydrocarbon phase. In a 'salting-out' variation of this assay, ammonium sulfate is incrementally added to the aqueous phase to enhance adhesion of bacteria to the hydrocarbon phase and thereby discriminate between the adhesion capabilities of bacteria that are hydrophilic (for example, the percentage of *E. coli* K-12 adhered to *n*-dodecane increases from 0.8% to 11% upon addition of ammonium sulfate; likewise, the percent adhesion to *p*-xylene increases from 0 to 67%) [63]. This example also reveals that solution conditions—choice of hydrocarbons, salt concentration, aqueous phase—sensitively affect the quantitative value extracted from the MATH assay, as also highlighted in Table 1. Given its simplicity, the MATH assay has been widely applied to characterize interactions of bacteria, including the known hydrocarbon degraders *Alcanivorax borkumensis* (3% of cells cultured under clean environmental conditions but 59% of those grown under hexadecane adhered to hexadecane in marine broth) [46] and *Marinobacter hydrocarbonoclasticus* (Table 1) [60];

Table 1 Mean and standard deviation for percent adhesion to hydrocarbon obtained from a MATH assay for marine bacteria under different solution conditions from the author's experiments

Bacterium	Hydrocarbon	Aqueous phase	Percent adhesion	Reference
Halomonas titanicae Bead 10BA	Dodecane	SSW	18 ± 5	[3]
Halomonas titanicae Bead 10BA	Hexadecane	SSW	26 ± 4	[3]
Halomonas titanicae Bead 10BA	Dodecane	0.9% NaCl	13 ± 1	[3]
Shewanella haliotis Bead B37B	Dodecane	SSW	55 ± 7	[3]
Marinobacter titanicae ATCC 49840	Dodecane	SSW	70 ± 2	[60]
Marinobacter titanicae ATCC 49840	Dodecane	SSW + 0.01CMC DOSS	54 ± 9	[60]
Marinobacter titanicae ATCC 49840	Dodecane	SSW + 0.01CMC Triton X-100	69 ± 1	[60]
Marinobacter titanicae ATCC 49840	Dodecane	SSW + 0.01CMC DOSS	68 ± 2	[60]

SSW synthetic sea water, *DOSS* dioctyl sodium sulfosuccinate, an anionic surfactant, *CTAB* cetyltrimethylammonium bromide, a cationic surfactant, *Triton-X-100* nonionic surfactant, *CMC* critical micelle concentration

the opportunistic pathogen *Pseudomonas aeruginosa* [64]; and several *Burkholderia* species (for which the percentage adhered to hexadecane decreased from ~ 60% at pH 2 to ~ 20 to 30% at pH 6) [65], at oil–water interfaces. Studies using the MATH assay have revealed, for example, that oil-degrading *Acinetobacter venetianus* RAG-1 and *Rhodococcus erythropolis* 20S-E1-c bacteria (96% and 90% adhesion to *n*-hexadecane, respectively) are able to stabilize oil-in-water emulsions by directly binding to the oil–water interface [66]. Similarly, MATH assays showed that addition of polycations to bacterial suspensions increases their apparent hydrophobicity (from near-zero adhesion to hexadecane to a maximum of ~60% in the presence of poly-L-lysine), due to the reduction in the electronegativity of the cell surface as cations bind there [67].

The MATH assay has also been used to examine how biological factors affect adhesion of bacteria on the oil–water interface. For example, *Acinetobacter venetianus* VE-C3 becomes hydrophobic (increase in percent adhesion to hexadecane from near-zero to 88%) only after exposure to alkanes, by incorporating nanodroplets of the alkane into its capsular polysaccharides [68]. For *Acinetobacter sp.* strain RAG-1, however, thin fimbriae control adhesion to alkanes [69]. Fimbriation also enables relatively hydrophilic bacteria (as assessed through the MATH assay) to more readily access oil–water interfaces. For example, *E. coli* is hydrophilic and typically exhibits weak adhesion to an oil–water interface (8% adhere to 1-dodecane in M63 medium) [70]. Overexpression of fimbriae in a strain with inducible fimbrial expression, however, greatly increases its adhesion to hydrocarbons (increase in adhesion to dodecane from 3% in wild type to 6% in the inducible strain with no inducer to a maximum of 24% upon induction) [71].

Although the MATH assay's simplicity has led to its widespread use, technical issues can complicate interpretation of the assay results. Careful control experiments are required to ensure that bacteria are not captured on the wall; in addition, use of a high-ionic strength buffer promotes adhesion of bacteria to the interface and minimizes electrostatic interactions [61]. Finally, the absorbance in the aqueous phase can also be increased by the presence of small, emulsified oil droplets in the aqueous phase, increasing the apparent hydrophobicity of the bacteria [72]. These limitations can in part be overcome through microscopic imaging (Section "Microscopy").

Rheometry

Rheological methods enable quantification of the mechanical properties of communities of bacteria at the oil–water interface. In pendant drop tensiometry, the interfacial tension between two liquids is extracted from the shape of the silhouette of an axisymmetric droplet dispensed from a needle via the Young–Laplace equation [73] (Fig. 2a). A decrease in the interfacial tension as a function of time may indicate that bacteria attach to the interface (Fig. 1b). This method can be extended to obtain the dilatational elastic modulus by applying a sinusoidal oscillation at the needle. Both methods were applied to examine the development of biofilms of *Marinobacter hydrocarbonoclasticus* SP17 at an alkane–water interface (Fig. 2b, c) [74]. The initial decrease of the interfacial tension over time for *M. hydrocarbonoclasticus* on both metabolizable and non-metabolizable alkane droplets suggests that adsorption is thermodynamically controlled by physicochemical factors. The elasticity of the interface, however, is greater on the metabolizable hexadecane, suggesting that the metabolic status of the cells affects the development of the elastic film [74]. Dynamic tensiometry experiments on hydrophobic *Acinetobacter venetianus* RAG-1, a highly efficient oil-degrading bacterium, and *Rhodococcus erythropolis* 20S-E1-c (both aerobic, non-motile, and metabolically versatile) reveal that the interfacial tension decrease is similar for both bacteria [75], again suggesting that adhesion is primarily controlled by thermodynamics.

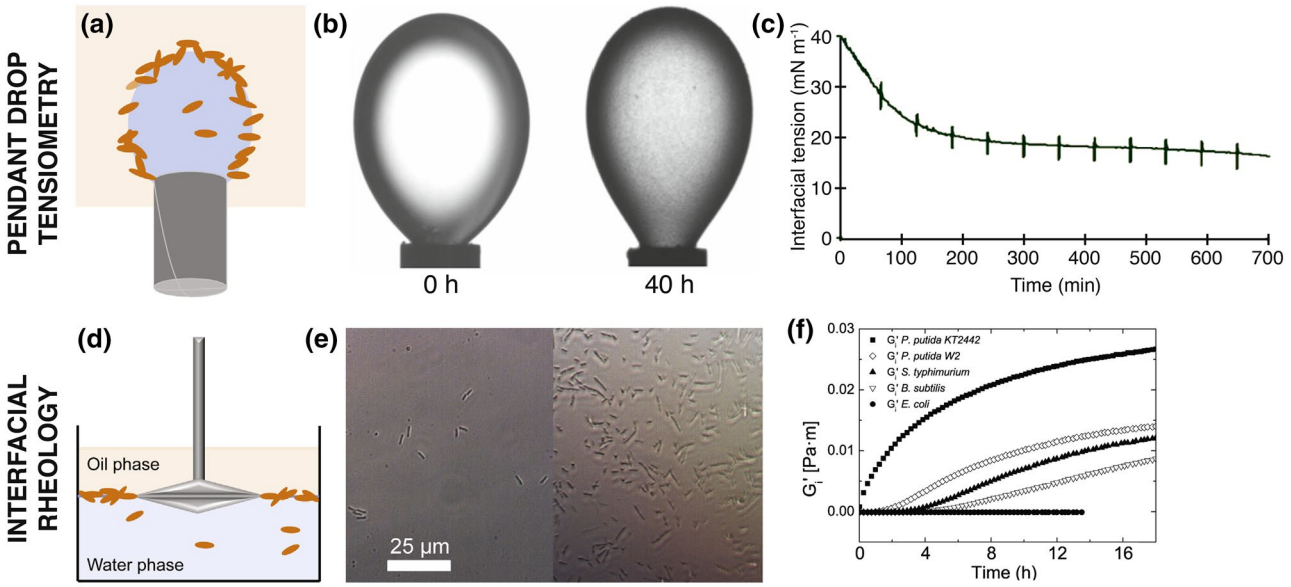

Fig. 2 **a** Schematic illustration of a pendant drop tensiometry experiment. **b** Images of hexadecane drops in suspensions of *M. hydrocarbonoclasticus*, showing the development of a biofilm as indicated by the increase in opacity over time. **c** Interfacial tension as a function of time for hexadecane in a suspension of *M. hydrocarbonoclasticus* in synthetic sea water. **d** Schematic illustration of an interfacial rheology experiment at the oil–water interface. **e** Brightfield micrographs of *E. coli*, left, and *P. putida* KT2442, right, at a mineral oil–water interface. **f** Time sweeps at constant amplitude $\gamma_s(t) = 0.5\%$ and frequency $\omega = 0.5\ s^{-1}$ for bacteria at the mineral oil–water interface. **a**, **d**, **e**, **f** reprinted from Ref. [78] with permission from Elsevier. **b**, **c** Adapted with permission from Ref. [74]

Different trends in the relaxation time upon a discontinuous step change in surface area, however, suggest that the cell–cell interactions dictate whether the interfacial film is able to resist in-plane shearing (as for *A. venetianus*) or is unable to resist shear (as for *R. erythropolis*) [75]. Strains of the opportunistic pathogen *Pseudomonas aeruginosa* exhibit different film-forming behaviors, as indicated by tensiometry: PAO1 forms elastic films even in the absence of flagella, pili, or the *pel* polysaccharide—all known to aid adhesion on solid surfaces [76]. The marine bacterium *Pseudomonas spp.* ATCC 27259, strain P62, exhibits three stages of film formation at the, sequentially active, viscoelastic, and elastic; the latter film wrinkles upon compression in tensiometry [77]. Together, these experiments reveal that bacteria can form films with various mechanical properties, which are dictated by interactions of bacteria with each other and with oil and water phases.

Rheological experiments can also be conducted using an interfacial shear cell, in which a tool is placed at the interface of two liquids (as in Ref. [79]). In a controlled shear instrument, a given rotation rate is applied and the resulting torque on the tool is measured; in a controlled stress instrument, a fixed stress is applied and the resulting rotation rate is measured. Rotating the tool unidirectionally enables measurements of the viscosity as a function of rotation rate or applied stress. By contrast, oscillating the tool (at a specified frequency and amplitude) enables measurements of elastic (G') and viscous (G'') moduli. Interfacial rheology experiments on bacteria most commonly measure the change in moduli over time ($G'(t)$ and $G''(t)$) to obtain information about biofilm development at the interface. Although more widely applied to air–water interfaces (e.g., for *Vibrio cholerae* [80] and *Pseudomonas aeruginosa* [81]), they have also been applied to oil–water interfaces. Measurements of the growth and attachment of five species (*Pseudomonas putida* KT2442, *P. putida* W2, *Salmonella typhimurium*, *Escherichia coli*, and *Bacillus subtilis*) at the mineral oil–water interface revealed that hydrophobic bacteria are more likely to form interfacial biofilms, but their biofilms were not necessarily more elastic [78] (Fig. 2f). Concomitant measurements of interfacial tension in this system suggested that elastic film development is more likely due to bacterial and protein adsorption rather than surfactant release [78].

Microscopy

The images in Fig. 2b, e suggest that differences in the mechanical properties of bacteria-coated oil–water interfaces arise from differences in the number and distribution of cells thereon. Both electron and optical microscopy techniques can be used to visualize cells at the oil–water interface. Scanning electron microscopy of bacteria [47, 48] and biofilms [76] at oil–water interfaces provides high spatial resolution but is not able to image living bacteria. Hence,

optical microscopy, which enables observations of living bacteria near the oil–water interface, is an essential tool for determining the interfacial location and density of bacteria. Both brightfield and fluorescence microscopy have been used to capture images of bacteria at interfaces (with examples in Refs. [46, 72]). These methods, however, are limited in their ability to examine 3D interfaces such as droplets; moreover, the resolution may be compromised by strong scattering arising from the mismatch in the index of refraction between bacteria and water or oil and water.

To overcome these limitations, confocal laser-scanning microscopy (CSLM) has been widely employed to image bacteria at oil–water interfaces. In CSLM, light emitted by a fluorophore in the focal plane of the excitation volume is captured through a pinhole, which blocks out-of-focus light; the focal point is then scanned rapidly to generate a virtual 2D or 3D image (Fig. 3). Judicious selection of fluorescent labels, required to generate a signal, allows cells, extracellular polysaccharides, or other structures of interest to be specifically labeled [82, 83]. Confocal micrographs revealed that the alkane-degrading bacterium *Rhodococcus erythropolis* is able to attach to the interface of alkane droplets, confirming that the bacteria themselves, and not simply biosurfactants that they may have released [84], are able to stabilize oil droplets in aqueous solutions [66]. Likewise, confocal micrographs of *Acenitobacter venetianus* VE-C3 revealed the small alkane nanodroplets that are incorporated into the matrix surrounding the cell to increase its hydrophobicity [68]. Subsequent studies showed that growth conditions modulate the ability to bacteria to adhere to the oil–water interface. For example, confocal imaging revealed that *A. borkumensis* cultured in the presence of hexadecane, mimicking an oil-spill condition, attaches to hexadecane interfaces more rapidly than those cultured using dissolved carbon [46]. Starting from an inoculum from contaminated soil, biofilms grow on droplets of polychlorinated biphenyl (PCB) oil suspended in water and, when mature, are able to degrade the PCBs [85]. Notably, many studies employing CSLM do not examine or characterize individual cells, even though the spatial resolution (typically, ~ 400 nm in-plane) is sufficient to resolve a single bacterium.

Single-cell studies in experiment and simulation

The techniques described in Section "Bulk methods" provide insight into bulk properties of bacteria at oil–water interfaces. Optical microscopy, however, also provides the necessary spatial resolution to resolve individual cells. Thus, these methods can also be applied in conjunction with computational algorithms to quantify the local behavior of bacteria, which may be heterogeneous even in a population of genetically identical bacteria [87]. Notably, this focus can provide the foundation needed to understand mechanisms affecting bacterial biodegradation of oil [49, 88]. In their simplest form, image-processing algorithms are applied to locate the centroids of micron-sized bacteria; subsequently, statistical

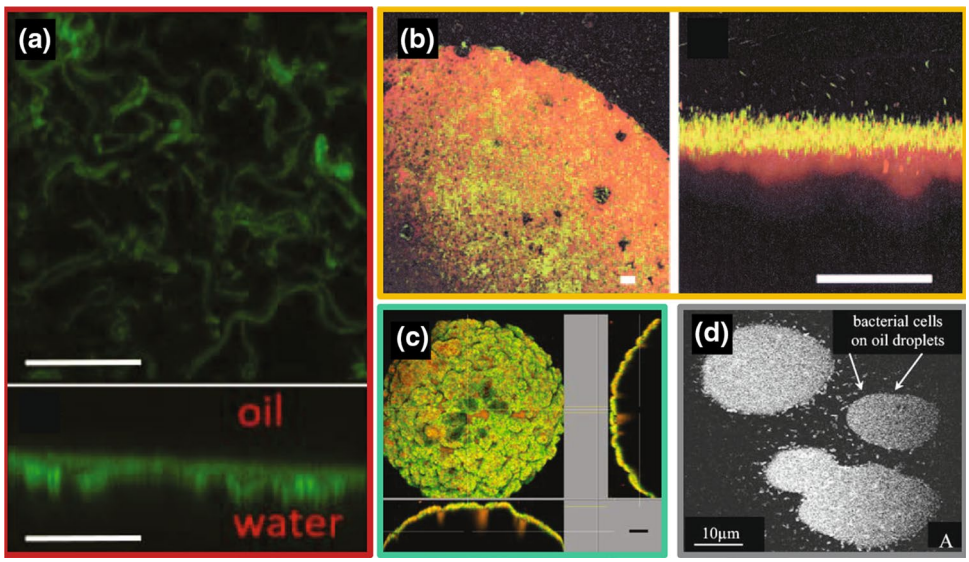

Fig. 3 Confocal micrographs of bacteria adhered to oil droplets in aqueous environments. **a** Top and side views of *A. borkumensis*. Reprinted with permission from Ref. [46]. Copyright (2018) American Chemical Society. **b** Top and side views of a mixed bacterial community. Reproduced from Ref. [85] with permission of the American Society for Microbiology. **c** Top and side views of *M. hydrocarbonoclasticus*. Reproduced with permission from Springer Nature from Ref. [86]. Copyright 2010. **d** Top view of *R. erythropolis* 20S-E1-c. Reproduced with permission from Ref. [66] with permission of the American Society for Microbiology

algorithms are used to link particle positions into trajectories based on minimization of total displacement [89]. High-throughput tracking techniques are widely applied to investigate bacterial motility [90–93], adhesion [94–99], and biofilm formation [100, 101] on solid substrates. They have also been applied to investigate the hydrodynamics [102] and accumulation [103–105] of swimming bacteria near solid surfaces.

Fewer studies, however, have examined bacterial behaviors near fluid–fluid interfaces, and most focus on air–liquid rather than liquid–liquid interfaces. Studies of swimming and accumulation are of fundamental interest because the no-stress boundary condition at a fluid–fluid interface can modify bacterial behaviors. For example, the difference in hydrodynamic drag on the top and bottom of a flagellum generates a wall-induced clockwise moment, which causes bacteria to swim in clockwise circles near a solid surface [106]. The slip boundary condition at the air–water interface, however, modifies the direction of the surface-induced moment, such that bacteria instead swim in counterclockwise circles [107]. As a second example, accounting for the compressibility of a surfactant-decorated air–water interface is required to predict the normal and tangential swimming speeds [108]. Thus, the physics of swimming is expected to be modified near oil–water interfaces.

Computational models complement single-cell experimental studies by allowing ranges of physical properties to be systematically varied. In the 'squirmer' model, swimming microorganisms are modeled as spheres swimming under conditions of low Reynolds number, in which viscous stresses dominate their motility [109]. Mathematically, many flagellated bacteria (e.g., the well-studied *E. coli*, a model bacterium for motility) generate extensile fluid flow along the axis of swimming. Such bacteria are commonly modeled to lowest order as 'pusher' force dipoles [110], arising from the balance of drag force from the body of a bacterium on the fluid and the countervailing thrust from the flagellum. Some monoflagellated bacteria (e.g., *P. aeruginosa* [111, 112] and *Vibrio alginolyticus* [113]), however, can switch the direction of rotation of the flagellum and exhibit 'puller' as well as 'pusher' behavior. 'Pullers' generate contractile flow along the axis of swimming, and are also modeled as dipoles of sign opposite that of pushers. Higher-order quadripolar terms in the force expansion, however, may need to be included to adequately describe the velocity correlations among swimming bacteria [114].

Here, we highlight insights into bacterial behaviors near oil–water interfaces that are gained from applying experimental and computational methods that give access to interactions of individual bacteria.

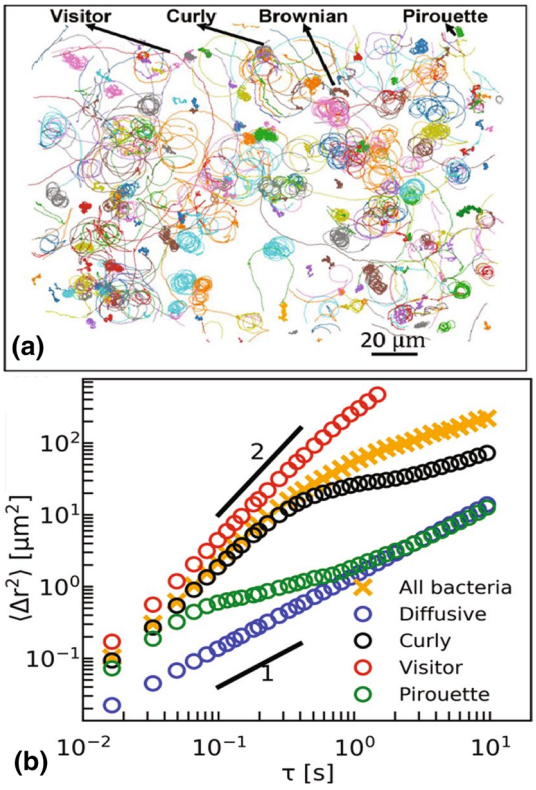

Fig. 4 **a** Trajectories of *P. aeruginosa* bacteria moving near a planar interface reveal four characteristic motility behaviors (visitor, diffusive, pirouette, or curly). **b** Mean-square displacement (MSD) as a function of time for *P. aeruginosa* bacteria exhibiting each of the four motility behaviors. The ensemble-average MSD is shown in yellow. Adapted with permission from Ref. [112]. Copyright (2020) American Chemical Society

Motility and accumulation near oil–water interfaces

The opportunistic pathogen *P. aeruginosa*, which bears one polar flagellum, can exhibit directed motion that enables it to accumulate at an oil–water interface [112] and transport cargo there [115]. Single-cell tracking of bacteria moving near a planar oil–water interface revealed four types of motility behaviors that can be distinguished through statistical analysis of the trajectories (Fig. 4a). Some bacteria briefly visit the interface and then leave ('visitor'). Other bacteria remain in the plane of the interface for at least 60 s. These bacteria diffuse passively ('diffusive') or swim in circular trajectories while oriented either perpendicular ('pirouette') or planar ('curly') with respect to the oil–water interface [115]. The motility behaviors produce differences in dispersal, as quantified through the ensemble-average mean-square displacement (MSD) $\left\langle \Delta r^2(t) \right\rangle$ (Fig. 4b). The MSD of diffusive bacteria scales linearly with time (i.e., MSD $\sim t$), as expected for micron-size particles undergoing random walks. Bacteria using other motility behaviors exhibit superdiffusive motion on short time scales, as indicated by

the scaling of the MSD ~ t^2 on short time scales, and transition to diffusive motion on long time scales. As a result, colloids attached to bacteria moving on the interface exhibit effective diffusivities that are up to fifty times greater than that of colloids freely diffusing at the interface [115]. Thus, motility behaviors can generate a wide range of bacterial transport coefficients at the oil–water interface.

Microscopic experiments on smooth-swimming (non-tumbling) *E. coli* revealed that bacteria accumulate more near a liquid–liquid or gas–liquid interface than predicted by theories developed for a solid–liquid interface. Moreover, accumulation is enhanced as the viscosity ratio between the two fluids is decreased [116]. Importantly, single-cell simulations incorporating both physicochemical and hydrodynamic interactions revealed that accumulation is due to a near-planar cell orientation near the interface [116]. Computational methods were also employed to quantify the distribution of microorganisms in a thin film of liquid that was confined on one side by air and by on the other by an immiscible liquid [117]. This geometry is a simplified representation of bacteria in an aqueous film near an oil phase, such as an oil slick found under spill conditions. Under the model conditions, the length of the flagella relative to the body length and the ratio of the viscosities of the two liquid phases determine whether bacteria accumulate near the liquid–liquid or liquid–air interface (Fig. 5) [117]. Surfactants cause interfaces to behave more like solids, so that surfactant-decorated oil–water interfaces may drive passive hydrodynamic trapping similar to that observed near a solid object [117]. Thus, these studies reveal that the interfacial hydrodynamics of a planar fluid–liquid interface affects the accumulation of bacteria there.

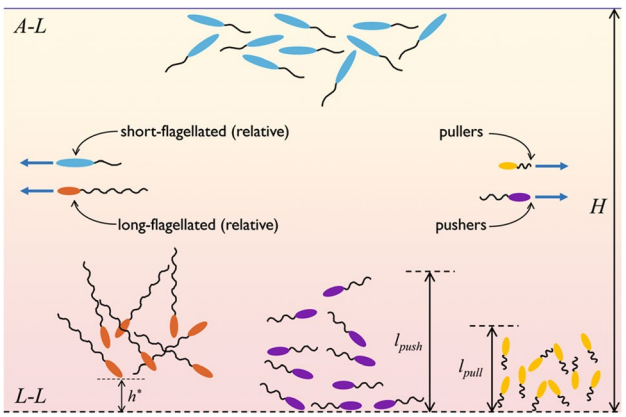

Fig. 5 Schematic illustration showing the properties that determine whether flagellated swimmers accumulate at the air–liquid (A–L) or liquid–liquid (L–L) interface. Swimmers with short flagella accumulate at A–L, whereas swimmers with long flagella accumulate near L–L. Pullers accumulate more tightly than pushers at all interfaces, as indicated by the shorter accumulation length over which bacteria accumulate (i.e. $l_{pull} < l_{push}$). Reproduced from Ref. [117] with permission from The Royal Society of Chemistry

Adhesion on oil–water interfaces

Finally, single-cell microscopy experiments demonstrated that both thermodynamic and kinetic factors affect adhesion of the oil-degrading marine bacterium *Marinobacter hydrocarbonoclasticus* SP17 bacteria to surfactant-decorated oil droplets [60]. The increase in the surface density of bacteria over time follows a first-order Langmuir kinetic model, in accord with results from bulk MATH assays [118], and depends weakly on droplet diameter. Most adhered bacteria align parallel to the surface, as expected through free-energy arguments for micron-sized particles [119]. Moreover, the long-time density obtained for droplets decorated with a variety of surfactants, including anionic sodium sulfosuccinates (such as DOSS), cationic CTAB, and non-ionic Tween-20, approximately collapses onto a single curve as a function of the interfacial tension. These results indicate that thermodynamics largely controls adhesion. Nonetheless, kinetic factors arising from electrostatic interactions also play a role in the long-time interfacial density, as revealed by the significant percentage (~ 30–40%) of bacteria that do not adopt the near-planar orientation predicted from free-energy arguments [60]. Thus, imaging methods suggest an additional barrier to adhesion arising from physicochemical interactions.

Despite possessing a flagellum, *M. hydrocarbonoclasticus* does not swim under the conditions of Ref. [60], and thus, the strong dependence of its adhesion on thermodynamics may be expected from earlier studies of micron-sized colloids at liquid–liquid interfaces [121]. Many marine bacteria, however, are able to swim and, additionally, may exhibit chemotaxis towards dispersed hydrocarbons [122, 123]. Single-cell CSLM experiments using the marine bacterium *Halomonas titanicae* (Fig. 6a, b) revealed that motile bacteria adhere more rapidly to the oil–water interface on short time scales and attain higher interfacial densities on long time scales (Fig. 6c) [120]. Both faster kinetics and higher density may enhance the formation of biofilms on the oil–water interface, thought to be the dominant strategy in nature for oil biodegradation [49]. Increasing the surfactant concentration reduces adhesion of both motile and nonmotile bacteria. Interestingly motile but not nonmotile bacteria are able to adhere to the oil–water interface even at very high surfactant concentrations [120], where the interfacial tension is very low.

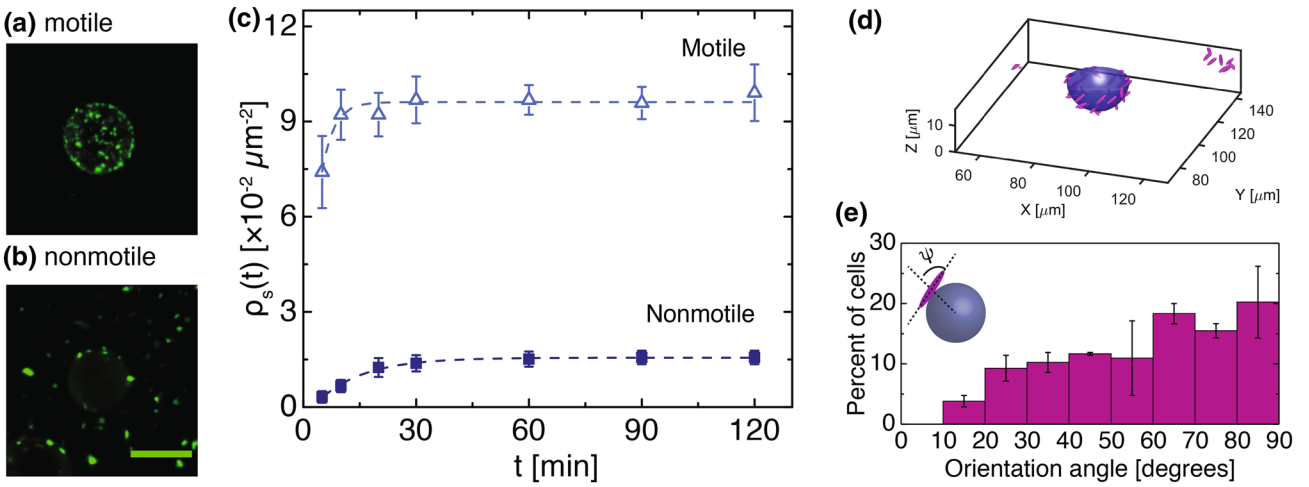

Fig. 6 **a**, **b** 2D projections of 3D confocal micrographs of **a** motile and **b** non-motile *H. titanicae* on hexadecane droplets of diameter 30 μm in synthetic sea water. **c** Interfacial density $\rho_s(t)$ as a function of time for *H. titanicae*. **d** Reconstructions of the orientation and location of *M. hydrocarbonoclasticus* bacteria on interface of hexadecane droplets of diameter 20 µm in saline solution. **e** Histograms of the orientation of bacteria located at the interface of hexadecane droplets of diameter 20 µm and **c** 60 µm in saline solution. An orientation ψ of 90° corresponds to a locally planar orientation. **d**, **e** Adapted with permission from Ref. [60]. Copyright (2018) American Chemical Society

Outlook: avenues to further microscopic understanding of biodegradation

Biophysical studies of bacterial behavior near oil–water interfaces have the opportunity to identify relevant physical phenomena that may significantly impact the efficacy of biodegradation processes in oil-spill response [14] as well as applications in biotechnology. Methods such as the MATH assay, rheology, and microscopy offer the ability to probe ensemble behaviors at oil–water interfaces and quantify cell hydrophobicity, mechanics, and distribution, respectively. Single-cell tracking experiments and computational simulations can enable the characterization of local or single-cell behaviors, and have led to insights into heterogeneous behaviors in motility, accumulation, and adhesion at oil–water interfaces.

Although there exist a variety of methods to assess bacterial behaviors at the oil–water interface, there remains a gap between biophysical studies and the microscopic understanding of biodegradation needed to remediate catastrophic oil spills. To bridge this gap, physical methods should be applied to examine the role of biological mechanisms—including but not limited to surface appendages [124, 125], extracellular polymers [126], and sensing pathways [127]—on bacterial interactions with the oil–water interface. Second, physical studies have focused on well-studied pathogenic bacteria such as *E. coli* and *P. aeruginosa*. Thus, application of these methods to both single-species cultures (including *Alcanivorax* and *Marinobacter*) as well as consortia of hydrocarbon-degrading bacteria has the potential to generate significant insight if they can be extended to the long time scales relevant for biofilm formation and biodegradation. These experiments should be carried out over a range of environmentally relevant conditions and with different hydrophobic substrates to broadly survey how these factors affect surfactant effects. The use of methods such as flow cytometry and fluorescence activated cell sorting [128–130] may provide a way to quantify metabolic activity [131] of individual bacteria in response to varying conditions. Finally, biodegradation processes in natural environments entail complex flows, as exemplified by the 'oil cloud' formed Corexit was applied at the DWH wellhead and subsequently transported through the Gulf. Extension of physical methods to gain insight into the effects of flows (including those driven by gradients in temperature or salinity in marine environments) [88] and confinement (by nearby droplets) [132] on bacterial interactions with dispersed oil will improve our ability to tailor and improve the emergency response for different environments.

Acknowledgements This research was made possible in part by a grant from The Gulf of Mexico Research Initiative, and in part by the Welch Foundation (E-1869).

References

1. Flemming HC, Wingender J, Szewzyk U, Steinberg P, Rice SA, Kjelleberg S (2016) Biofilms: an emergent form of bacterial

life. Nat Rev Microbiol 14:563. https://doi.org/10.1038/nrmicro.2016.94
2. Abbasnezhad H, Gray M, Foght JM (2011) Influence of adhesion on aerobic biodegradation and bioremediation of liquid hydrocarbons. Appl Microbiol Biotechnol 92:653. https://doi.org/10.1007/s00253-011-3589-4
3. Dewangan NK, Conrad JC (2019) Rotating oil droplets driven by motile bacteria at interfaces. Soft Matter 15:9368. https://doi.org/10.1039/C9SM01570A
4. Ramos G, Cordero ML, Soto R (2020) Bacteria driving droplets. Soft Matter 16:1359. https://doi.org/10.1039/C9SM01839E
5. Rühs PA, Storz F, López Gómez YA, Haug M, Fischer P (2018) 3D bacterial cellulose biofilms formed by foam templating. npj Biofilms Microbiomes 4:21. https://doi.org/10.1038/s41522-018-0064-3
6. Brooijmans RJ, Pastink MI, Siezen RJ (2009) Hydrocarbon-degrading bacteria: the oil-spill clean-up crew. Microb Biotechnol 2(6):587. https://doi.org/10.1111/j.1751-7915.2009.00151.x
7. Hazen TC, Dubinsky EA, DeSantis TZ, Andersen GL, Piceno YM, Singh N, Jansson JK, Probst A, Borglin SE, Fortney JL, Stringfellow WT, Bill M, Conrad ME, Tom LM, Chavarria KL, Alusi TR, Lamendella R, Joyner DC, Spier C, Baelum J, Auer M, Zemla ML, Chakraborty R, Sonnenthal EL, D'haeseleer P, Holman HYN, Osman S, Lu Z, Van Nostrand JD, Deng Y, Zhou J, Mason OU (2010) Deep-sea oil plume enriches indigenous oil-degrading bacteria. Science 330(6001):204. https://doi.org/10.1126/science.1195979
8. Valentine DL, Kessler JD, Redmond MC, Mendes SD, Heintz MB, Farwell C, Hu L, Kinnaman FS, Yvon-Lewis S, Du M, Chan EW, Tigreros FG, Villanueva CJ (2010) Propane respiration jump-starts microbial response to a deep oil spill. Science 330(6001):208. https://doi.org/10.1126/science.1196830
9. Kostka JE, Prakash O, Overholt WA, Green SJ, Freyer G, Canion A, Delgardio J, Norton N, Hazen TC, Huettel M (2011) Hydrocarbon-degrading bacteria and the bacterial community response in Gulf of Mexico beach sands impacted by the Deepwater Horizon oil spill. Appl Environ Microbiol 77(22):7962. https://doi.org/10.1128/AEM.05402-11
10. Kessler JD, Valentine DL, Redmond MC, Du M, Chan EW, Mendes SD, Quiroz EW, Villanueva CJ, Shusta SS, Werra LM, Yvon-Lewis SA, Weber TC (2011) A persistent oxygen anomaly reveals the fate of spilled methane in the deep Gulf of Mexico. Science 331(6015):312. https://doi.org/10.1126/science.1199697
11. King G, Kostka J, Hazen T, Sobecky P (2015) Microbial responses to the Deepwater Horizon oil spill: from coastal wetlands to the deep sea. Annu Rev Mar Sci 7(1):377. https://doi.org/10.1146/annurev-marine-010814-015543
12. Crone TJ, Tolstoy M (2010) Magnitude of the 2010 Gulf of Mexico oil leak. Science 330(6004):634. https://doi.org/10.1126/science.1195840
13. Graham LJ, Hale C, Maung-Douglass E, Sempier S, Swann L, Wilson M (2016) Chemical dispersants and their role in oil spill response. Oil Spill Sci. Sea Grant Programs Gulf Mex, p 1
14. National Academies of Sciences, Engineering, and Medicine (2020) The use of dispersants in marine oil spill response. The National Academies Press, Washington, DC. https://doi.org/10.17226/25161
15. Prince RC (2015) Oil spill dispersants: boon or bane? Environ Sci Technol 49(11):6376. https://doi.org/10.1021/acs.est.5b00961
16. McFarlin KM, Prince RC, Perkins R, Leigh MB (2014) Biodegradation of dispersed oil in Arctic Seawater at -1°C. PLos One 9(1):e84297. https://doi.org/10.1371/journal.pone.0084297
17. National Research Council (2005) Oil spill dispersants: efficacy and effects. The National Academies Press, Washington, DC. https://doi.org/10.17226/11283
18. Riehm DA, Rokke DJ, McCormick AV (2016) Water-in-oil microstructures formed by marine oil dispersants in a model crude oil. Langmuir 32(16):3954. https://doi.org/10.1021/acs.langmuir.6b00643
19. Li C, Miller J, Wang J, Koley SS, Katz J (2017) Size distribution and dispersion of droplets generated by impingement of breaking waves on oil slicks. J Geophys Res Oceans 122(10):7938. https://doi.org/10.1002/2017JC013193
20. Li Z, Lee K, Kepkey PE, Mikkelsen O, Pottsmith C (2011) Monitoring dispersed oil droplet size distribution at the Gulf of Mexico Deepwater Horizon spill site. In: International oil spill conference proceedings, abs377. https://doi.org/10.7901/2169-3358-2011-1-377
21. Camilli R, Reddy CM, Yoerger DR, Van Mooy BAS, Jakuba MV, Kinsey JC, McIntyre CP, Sylva SP, Maloney JV (2010) Tracking hydrocarbon plume transport and biodegradation at deepwater horizon. Science 330(6001):201. https://doi.org/10.1126/science.1195223
22. Atlas RM, Hazen TC (2011) Oil biodegradation and bioremediation: a tale of the two worst spills in U.S. History. Environ Sci Technol 45(16):6709. https://doi.org/10.1021/es2013227
23. The Federal Interagency Solutions Group: Oil Budget Calculator Science and Engineering Team. Oil budget calculator technical documentation. http://www.restorethegulf.gov/sites/default/files/documents/pdf/OilBudgetCalc_Full_HQ-Print_111110.pdf. Accessed 6 July 2020
24. North EW, Adams EE, Thessen AE, Schlag Z, He R, Socolofsky SA, Masutani SM, Peckham SD (2015) The influence of droplet size and biodegradation on the transport of subsurface oil droplets during the Deepwater Horizon spill: a model sensitivity study. Environ Res Lett 10(2):024016. https://doi.org/10.1088/1748-9326/10/2/024016
25. Ron EZ, Rosenberg E (2002) Biosurfactants and oil bioremediation. Curr Opin Biotechnol 13(3):249. https://doi.org/10.1016/S0958-1669(02)00316-6
26. Karlapudi AP, Venkateswarulu T, Tammineedi J, Kanumuri L, Ravuru BK, ramu Dirisala V, Kodali VP, (2018) Role of biosurfactants in bioremediation of oil pollution-a review. Petroleum 4(3):241. https://doi.org/10.1016/j.petlm.2018.03.007
27. Schwehr KA, Xu C, Chiu MH, Zhang S, Sun L, Lin P, Beaver M, Jackson C, Agueda O, Bergen C, Chin WC, Quigg A, Santschi PH (2018) Protein: polysaccharide ratio in exopolymeric substances controlling the surface tension of seawater in the presence or absence of surrogate Macondo oil with and without Corexit. Mar Chem 206:84. https://doi.org/10.1016/j.marchem.2018.09.003
28. White AR, Jalali M, Boufadel MC, Sheng J (2020) Bacteria forming drag-increasing streamers on a drop implicates complementary fates of rising deep-sea oil droplets. Sci Rep 10:4305. https://doi.org/10.1038/s41598-020-61214-9
29. White AR, Jalali M, Sheng J (2020) Hydrodynamics of a rising oil droplet with bacterial extracellular polymeric substance (EPS) streamers using a microfluidic microcosm. Front Mar Sci 7:294. https://doi.org/10.3389/fmars.2020.00294
30. Desai N, Dabiri S, Ardekani AM (2018) Nutrient uptake by chemotactic bacteria in presence of rising oil drops. Int J Multiphase Flow 108:156. https://doi.org/10.1016/j.ijmultiphaseflow.2018.06.016
31. Kleindienst S, Seidel M, Ziervogel K, Grim S, Loftis K, Harrison S, Malkin SY, Perkins MJ, Field J, Sogin ML, Dittmar T, Passow U, Medeiros PM, Joye SB (2015) Chemical dispersants can suppress the activity of natural oil-degrading microorganisms.

Proc Natl Acad Sci 112(48):14900. https://doi.org/10.1073/pnas.1507380112
32. Kleindienst S, Grim S, Sogin M, Bracco A, Crespo-Medina M, Joye SB (2016) Diverse, rare microbial taxa responded to the Deepwater Horizon deep-sea hydrocarbon plume. ISME J 10:400. https://doi.org/10.1038/ismej.2015.121
33. Hamdan LJ, Fulmer PA (2011) Effects of COREXIT® EC9500A on bacteria from a beach oiled by the Deepwater Horizon spill. Aquat Microb Ecol 63(2):101. https://doi.org/10.3354/ame01482
34. Sun X, Chu L, Mercando E, Romero I, Hollander D, Kostka JE (2019) Dispersant enhances hydrocarbon degradation and alters the structure of metabolically active microbial communities in shallow seawater from the Northeastern Gulf of Mexico. Front Microbiol 10:2387. https://doi.org/10.3389/fmicb.2019.02387
35. Bælum J, Borglin S, Chakraborty R, Fortney JL, Lamendella R, Mason OU, Auer M, Zemla M, Bill M, Conrad ME, Malfatti SA, Tringe SG, Holman HY, Hazen TC, Jansson JK (2012) Deep-sea bacteria enriched by oil and dispersant from the Deepwater Horizon spill. Environ Microbiol 14(9):2405. https://doi.org/10.1111/j.1462-2920.2012.02780.x
36. Tremblay J, Yergeau E, Fortin N, Cobanli S, Elias M, Tl King, Lee K, Greer CW (2017) Chemical dispersants enhance the activity oof oil- and gas condensate-degrading marine bacteria. ISME J 11:2793. https://doi.org/10.1038/ismej.2017.129
37. Mulkins-Phillips GJ, Stewart JE (1974) Effect of four dispersants on biodegradation and growth of bacteria on crude oil. Appl Microbiol 28:547. https://aem.asm.org/content/aem/28/4/547.full.pdf
38. Techtmann SM, Zhuang M, Campo P, Holder E, Elk M, Hazen TC, Conmy R, Santo Domingo JW (2017) Corexit 9500 enhances oil biodegradation and changes active bacterial community structure of oil-enriched microcosms. Appl Environ Microbiol 83(10):e03462-16. https://doi.org/10.1128/AEM.03462-16
39. Daly KL, Passow U, Chanton J, Hollander D (2016) Assessing the impacts of oil-associated marine snow formation and sedimentation during and after the Deepwater Horizon oil spill. Anthropocene 13:18. https://doi.org/10.1016/j.ancene.2016.01.006
40. Quigg A, Passow U, Daly KL, Burd A, Hollander DJ, Schwing PT, Lee K (2020) Marine oil snow sedimentation and flocculent accumulation (MOSSFA) events: learning from the past to predict the future. In: Murawski S et al (eds) Deep oil spills. Springer, Cham
41. Passow U, Ziervogel K, Asper V, Diercks A (2012) Marine snow formation in the aftermath of the Deepwater Horizon oil spill in the Gulf of Mexico. Environ Res Lett 7(3):035301. https://doi.org/10.1088/1748-9326/7/3/035301
42. Fu J, Gong Y, Zhao X, O'reilly SE, Zhao D (2014) Effects of oil and dispersant on formation of marine oil snow and transport of oil hydrocarbons. Environ Sci Technol 48(24):14392. https://doi.org/10.1021/es5042157
43. Passow U, Sweet J, Quigg A (2017) How the dispersant Corexit impacts the formation of sinking marine oil snow. Mar Pollut Bull 125(1):139. https://doi.org/10.1016/j.marpolbul.2017.08.015
44. Suja LD, Chen X, Summers S, Paterson DM, Gutierrez T (2019) Chemical dispersant enhances microbial exopolymer (EPS) production and formation of marine oil/dispersant snow in surface waters of the subarctic Northeast Atlantic. Front Microbiol 10:553. https://doi.org/10.3389/fmicb.2019.00553
45. Bookstaver M, Bose A, Tripathi A (2015) Interaction of *Alcanivorax borkumensis* with a surfactant decorated oil-water interface. Langmuir 31(21):5875. https://doi.org/10.1021/acs.langmuir.5b00688
46. Godfrin MP, Sihlabela M, Bose A, Tripathi A (2018) Behavior of marine bacteria in clean environment and oil spill conditions. Langmuir 34(30):9047. https://doi.org/10.1021/acs.langmuir.8b01319
47. Abbasi A, Bothun GD, Bose A (2018) Attachment of *Alcanivorax borkumensis* to hexadecane-in-artificial sea water emulsion droplets. Langmuir 34(18):5352. https://doi.org/10.1021/acs.langmuir.8b00082
48. Omarova M, Swientoniewski LT, Mkam Tsengam IK, Blake DA, John V, McCormick A, Bothun GD, Raghavan SR, Bose A (2019) Biofilm formation by hydrocarbon-degrading marine bacteria and its effects on oil dispersion. ACS Sustain Chem Eng 7(17):14490. https://doi.org/10.1021/acssuschemeng.9b01923
49. Kapellos G (2017) Chapter 2-microbial strategies for oil biodegradation. In: Becker SM (ed) Modeling of microscale transport in biological processes. Academic Press, pp 19–39. https://doi.org/10.1016/B978-0-12-804595-4.00002-X
50. Vergeynst L, Wegeberg S, Aamand J, Lassen P, Gosewinkel U, Fritt-Rasmussen J, Gustavson K, Mosbech A (2018) Biodegradation of marine oil spills in the Arctic with a Greenland perspective. SciTotal Environ 626:1243. https://doi.org/10.1016/j.scitotenv.2018.01.173
51. Krasowska A, Sigler K (2014) How microorganisms use hydrophobicity and what does this mean for human needs? Front Cell Infect Microbiol 4:112. https://doi.org/10.3389/fcimb.2014.00112
52. Alexander TE, Lozeau LD, Camesano TA (2019) QCM-D characterization of time-dependence of bacterial adhesion. Cell Surf 5:100024. https://doi.org/10.1016/j.tcsw.2019.100024
53. Dufrêne YF (2014) Atomic force microscopy in microbiology: new structural and functional insights into the microbial cell surface. mBio 5(4):e01363-14. https://doi.org/10.1128/mBio.01363-14
54. Wick LY, Pasche N, Bernasconi SM, Pelz O, Harms H (2003) Characterization of multiple-substrate utilization by anthracene-degrading *Mycobacterium frederiksbergense* LB501T. Appl Environ Microbiol 69(10):6133. https://doi.org/10.1128/AEM.69.10.6133-6142.2003
55. Wu S (1971) Calculation of interfacial tensions in polymer systems. J Polym Sci 43:19. https://doi.org/10.1002/polc.5070340105
56. Owens D, Wendt R (1969) Estimation of the surface free energy of polymers. J Appl Polym Sci 13:1741. https://doi.org/10.1002/app.1969.070130815
57. Kaelble DH (1970) Dispersion-polar surface tension properties of organic solids. J Adhes 2:66. https://doi.org/10.1080/00218467085445 82
58. Rabel W (1971) Einige Aspekte der Benetzungstheorie und ihre Anwendung auf die Untersuchung und Veränderung der Oberflächeneigenschaften von Polymeren. Farbe Lack 77:997
59. Tuson HH, Weibel DB (2013) Bacteria-surface interactions. Soft Matter 9:4368. https://doi.org/10.1039/C3SM27705D
60. Dewangan NK, Conrad JC (2018) Adhesion of *Marinobacter hydrocarbonoclasticus* to surfactant-decorated dodecane droplets. Langmuir 34(46):14012. https://doi.org/10.1021/acs.langmuir.8b02071
61. Rosenberg M (2006) Microbial adhesion to hydrocarbons: twenty-five years of doing MATH. FEMS Microbiol Lett 262(2):129. https://doi.org/10.1111/j.1574-6968.2006.00291.x
62. Rosenberg M (1984) Bacterial adherence to hydrocarbons: a useful technique for studying cell surface hydrophobicity. FEMS Microbiol Lett 22(3):289. https://doi.org/10.1111/j.1574-6968.1984.tb00743.x
63. Rosenberg M (1984) Ammonium sulphate enhances adherence of *Escherichia coli* J-5 to hydrocarbon and polystyrene. FEMS Microbiol Lett 25(1):41. https://doi.org/10.1111/j.1574-6968.1984.tb01372.x

64. Zoueki CW, Ghoshal S, Tufenkji N (2010) Bacterial adhesion to hydrocarbons: role of asphaltenes and resins. Colloids Surf B Biointerfaces 79(1):219. https://doi.org/10.1016/j.colsurfb.2010.03.054
65. Chakraborty S, Mukherji S, Mukherji S (2010) Surface hydrophobicity of petroleum hydrocarbon degrading *Burkholderia* strains and their interactions with NAPLs and surfaces. Colloids Surf B Biointerfaces 78(1):101. https://doi.org/10.1016/j.colsurfb.2010.02.019
66. Dorobantu LS, Yeung AKC, Foght JM, Gray MR (2004) Stabilization of oil-water emulsions by hydrophobic bacteria. Appl Environ Microbiol 70(10):6333. https://doi.org/10.1128/AEM.70.10.6333-6336.2004
67. Goldberg S, Doyle RJ, Rosenberg M (1990) Mechanism of enhancement of microbial cell hydrophobicity by cationic polymers. J Bacteriol 172(10):5650. https://doi.org/10.1128/jb.172.10.5650-5654.1990
68. Baldi F, Ivošević N, Minacci A, Pepi M, Fani R, Svetličić V, Žutić V (1999) Adhesion of *Acinetobacter venetianus* to diesel fuel droplets studied with in situ electrochemical and molecular probes. Appl Environ Microbiol 65(5):2041. https://doi.org/10.1128/AEM.65.5.2041-2048.1999
69. Rosenberg M, Bayer EA, Delarea J, Rosenberg E (1982) Role of thin fimbriae in adherence and growth of *Acinetobacter calcoaceticus* RAG-1 on hexadecane. Appl Environ Microbiol 44(4):929
70. Rodrigues DF, Elimelech M (2009) Role of type 1 fimbriae and mannose in the development of *Escherichia coli* K12 biofilm: from initial cell adhesion to biofilm formation. Biofouling 25(5):401. https://doi.org/10.1080/08927010902833443
71. McLay RB, Nguyen HN, Jaimes-Lizcano YA, Dewangan NK, Alexandrova S, Rodrigues DF, Cirino PC, Conrad JC (2018) Level of fimbriation alters the adhesion of *Escherichia coli* bacteria to interfaces. Langmuir 34(3):1133. https://doi.org/10.1021/acs.langmuir.7b02447
72. Zoueki CW, Tufenkji N, Ghoshal S (2010) A modified microbial adhesion to hydrocarbons assay to account for the presence of hydrocarbon droplets. J Colloid Interface Sci 344(2):492. https://doi.org/10.1016/j.jcis.2009.12.043
73. Berry JD, Neeson MJ, Dagastine RR, Chan DY, Tabor RF (2015) Measurement of surface and interfacial tension using pendant drop tensiometry. J Colloid Interface Sci 454:226. https://doi.org/10.1016/j.jcis.2015.05.012
74. Klein B, Bouriat P, Goulas P, Grimaud R (2010) Behavior of *Marinobacter hydrocarbonoclasticus* SP17 cells during initiation of biofilm formation at the alkane-water interface. Biotechnol Bioeng 105(3):461. https://doi.org/10.1002/bit.22577
75. Kang Z, Yeung A, Foght JM, Gray MR (2008) Mechanical properties of hexadecane-water interfaces with adsorbed hydrophobic bacteria. Colloids Surf B Biointerfaces 62(2):273. https://doi.org/10.1016/j.colsurfb.2007.10.021
76. Niepa THR, Vaccari L, Leheny RL, Goulian M, Lee D, Steve KJ (2017) Films of bacteria at interfaces (FBI): remodeling of fluid interfaces by *Pseudomonas aeruginosa*. Sci Rep 7:17864. https://doi.org/10.1038/s41598-017-17721-3
77. Vaccari L, Allan DB, Sharifi-Mood N, Singh AR, Leheny RL, Stebe KJ (2015) Films of bacteria at interfaces: three stages of behaviour. Soft Matter 11:6062. https://doi.org/10.1039/C5SM00696A
78. Rühs P, Böcker L, Inglis R, Fischer P (2014) Studying bacterial hydrophobicity and biofilm formation at liquid-liquid interfaces through interfacial rheology and pendant drop tensiometry. Colloids Surf B Biointerfaces 117:174. https://doi.org/10.1016/j.colsurfb.2014.02.023
79. Lin YJ, Barman S, He P, Zhang Z, Christopher GF, Biswal SL (2018) Combined interfacial shear rheology and microstructure visualization of asphaltenes at air-water and oil-water interfaces. J Rheol 62(1):1. https://doi.org/10.1122/1.5009188
80. Hollenbeck EC, Fong JCN, Lim JY, Yildiz FH, Fuller GG, Cegelski L (2014) Molecular determinants of mechanical properties of *V. cholerae* biofilms at the air-liquid interface. Biophys J 107:2245. https://doi.org/10.1016/j.bpj.2014.10.015
81. Qi L, Christopher GF (2019) Role of flagella, type IV pili, biosurfactants, and extracellular polymeric substance polysaccharides on the formation of pellicles by *Pseudomonas aeruginosa*. Langmuir 35(15):5294. https://doi.org/10.1021/acs.langmuir.9b00271
82. Schlafer S, Meyer RL (2017) Confocal microscopy imaging of the biofilm matrix. What's next in microbiology methods? Emerging methods. J Microbiol Methods 138:50. https://doi.org/10.1016/j.mimet.2016.03.002
83. Reichhardt C, Parsek MR (2019) Confocal laser scanning microscopy for analysis of *Pseudomonas aeruginosa* biofilm architecture and matrix localization. Front Microbiol 10:677. https://doi.org/10.3389/fmicb.2019.00677
84. Reddy PG, Singh HD, Roy PK, Baruah JN (1982) Predominant role of hydrocarbon solubilization in the microbial uptake of hydrocarbons. Biotechnol Bioeng 24(6):1241. https://doi.org/10.1002/bit.260240603
85. Macedo AJ, Kuhlicke U, Neu TR, Timmis KN, Abraham WR (2005) Three stages of a biofilm community developing at the liquid-liquid interface between polychlorinated biphenyls and water. Appl Environ Microbiol 71(11):7301. https://doi.org/10.1128/AEM.71.11.7301-7309.2005
86. Grimaud R (2010) Biofilm development at interfaces between hydrophobic organic compounds and water. In: Timmis KN (ed) Handbook of hydrocarbon and lipid microbiology. Springer, Berlin, Heidelberg. https://doi.org/10.1007/978-3-540-77587-4_102
87. Davis KM, Isberg RR (2016) Defining heterogeneity within bacterial populations via single cell approaches. BioEssays 38(8):782. https://doi.org/10.1002/bies.201500121
88. Stocker R (2012) Marine microbes see a sea of gradients. Science 338(6107):628. https://doi.org/10.1126/science.1208929
89. Crocker JC, Grier DG (1996) Methods of digital video microscopy for colloidal studies. J Colloid Interface Sci 179(1):298. https://doi.org/10.1006/jcis.1996.0217
90. Gibiansky ML, Conrad JC, Jin F, Gordon VD, Motto DA, Mathewson MA, Stopka WG, Zelasko DC, Shrout JD, Wong GCL (2010) Bacteria use type IV pili to walk upright and detach from surfaces. Science 330(6001):197. https://doi.org/10.1126/science.1194238
91. Conrad JC, Gibiansky ML, Jin F, Gordon VD, Motto DA, Mathewson MA, Stopka WG, Zelasko DC, Shrout JD, Wong GCL (2011) Flagella and pili-mediated near-surface single-cell motility mechanisms in *P. aeruginosa*. Biophys J 100(7):1608. https://doi.org/10.1016/j.bpj.2011.02.020
92. Jin F, Conrad JC, Gibiansky ML, Wong GCL (2011) Bacteria use type-IV pili to slingshot on surfaces. Proc Natl Acad Sci 108(31):12617. https://doi.org/10.1073/pnas.1105073108
93. de Anda J, Lee EY, Lee CK, Bennett RR, Ji X, Soltani S, Harrison MC, Baker AE, Luo Y, Chou T, O'Toole GA, Armani AM, Golestanian R, Wong GCL (2017) High-Speed "4D" computational microscopy of bacterial surface motility. ACS Nano 11(9):9340. https://doi.org/10.1021/acsnano.7b04738
94. Vigeant MAS, Ford RM, Wagner M, Tamm LK (2002) Reversible and irreversible adhesion of motile *Escherichia coli* cells analyzed by total internal reflection aqueous fluorescence microscopy. Appl Environ Microbiol 68(6):2794. https://doi.org/10.1016/j.bpj.2011.02.020
95. De La Fuente L, Montanes E, Meng Y, Li Y, Burr TJ, Hoch HC, Wu M (2007) Assessing adhesion forces of type i and type iv pili of *Xylella fastidiosa* bacteria by use of a microfluidic

flow chamber. Appl Environ Microbiol 73(8):2690. https://doi.org/10.1128/AEM.02649-06
96. Sharma S, Conrad JC (2014) Attachment from flow of *Escherichia coli* bacteria onto silanized glass substrates. Langmuir 30(37):11147. https://doi.org/10.1021/la502313y
97. Song L, Sjollema J, Sharma PK, Kaper HJ, van der Mei HC, Busscher HJ (2014) Nanoscopic vibrations of bacteria with different cell-wall properties adhering to surfaces under flow and static conditions. ACS Nano 8(8):8457. https://doi.org/10.1021/nn5030253
98. Cooley BJ, Dellos-Nolan S, Dhamani N, Todd R, Waller W, Wozniak D, Gordon VD (2016) Asymmetry and inequity in the inheritance of a bacterial adhesive. New J Phys 18(4):045019. https://doi.org/10.1088/1367-2630/18/4/045019
99. Sharma S, Jaimes-Lizcano YA, McLay RB, Cirino PC, Conrad JC (2016) Subnanometric roughness affects the deposition and mobile adhesion of *Escherichia coli* on silanized glass surfaces. Langmuir 32(21):5422. https://doi.org/10.1021/acs.langmuir.6b00883
100. Drescher K, Dunkel J, Nadell CD, van Teeffelen S, Grnja I, Wingreen NS, Stone HA, Bassler BL (2016) Architectural transitions in *Vibrio cholerae* biofilms at single-cell resolution. Proc Natl Acad Sci 113(14):E2066. https://doi.org/10.1073/pnas.1601702113
101. Pearce P, Song B, Skinner DJ, Mok R, Hartmann R, Singh PK, Jeckel H, Oishi JS, Drescher K, Dunkel J (2019) Flow-induced symmetry breaking in growing bacterial biofilms. Phys Rev Lett 123:258101. https://doi.org/10.1103/PhysRevLett.123.258101
102. DiLuzio WR, Turner L, Mayer M, Garstecki P, Weibel DB, Berg HC, Whitesides GM (2005) *Escherichia coli* swim on the right hand side. Nature 435:1271. https://doi.org/10.1038/nature03660
103. Berke AP, Turner L, Berg HC, Lauga E (2008) Hydrodynamic attraction of swimming microorganisms by surfaces. Phys Rev Lett 101:038102. https://doi.org/10.1103/PhysRevLett.101.038102
104. Li G, Tang JX (2009) Accumulation of microswimmers near a surface mediated by collision and rotational Brownian motion. Phys Rev Lett 103(7):078101. https://doi.org/10.1103/PhysRevLett.103.078101
105. Bianchi S, Saglimbeni F, Di Leonardo R (2017) Holographic imaging reveals the mechanism of wall entrapment in swimming bacteria. Phys Rev X 7(1):011010. https://doi.org/10.1103/PhysRevX.7.011010
106. Lauga E, DiLuzio WR, Whitesides GM, Stone HA (2006) Swimming in circles: motion of bacteria near solid boundaries. Biophys J 90(2):400. https://doi.org/10.1529/biophysj.105.069401
107. Di Leonardo R, Dell'Arciprete D, Angelani L, Iebba V (2011) Swimming with an Image. Phys Rev Lett 106:038101. https://doi.org/10.1103/PhysRevLett.106.038101
108. Bianchi S, Saglimbeni F, Frangipane G, Dell'Arciprete D, Di Leonardo R (2019) 3D dynamics of bacteria wall entrapment at a water-air interface. Soft Matter 15:3397. https://doi.org/10.1039/C9SM00077A
109. Lighthill MJ (1952) On the squirming motion of nearly spherical deformable bodies through liquids at very small Reynolds numbers. Commun Pure Appl Math 5(2):109. https://doi.org/10.1002/cpa.3160050201
110. Lauga E, Powers TR (2009) The hydrodynamics of swimming microorganisms. Rep Prog Phys 72(9):096601. https://doi.org/10.1088/0034-4885/72/9/096601
111. Qian C, Wong CC, Swarup S, Chiam KH (2013) Bacterial tethering analysis reveals a "Run-Reverse-Turn" mechanism for Pseudomonas species motility. Appl Environ Microbiol 79(15):4734. https://doi.org/10.1128/AEM.01027-13
112. Deng J, Molaei M, Chisholm NG, Stebe KJ (2020) Motile bacteria at oil-water interfaces: *Pseudomonas aeruginosa*. Langmuir 36(25):6888. https://doi.org/10.1021/acs.langmuir.9b03578
113. Wu KT, Hsiao YT, Woon WY (2018) Entrapment of pusher and puller bacteria near a solid surface. Phys Rev E 98:052407. https://doi.org/10.1103/PhysRevE.98.052407
114. Liao Q, Subramanian G, DeLisa MP, Koch DL, Wu M (2007) Pair velocity correlations among swimming *Escherichia coli* bacteria are determined by force-quadrupole hydrodynamic interactions. Phys Fluids 19(6):061701. https://doi.org/10.1063/1.2742423
115. Vaccari L, Molaei M, Leheny RL, Stebe KJ (2018) Cargo carrying bacteria at interfaces. Soft Matter 14:5643. https://doi.org/10.1039/C8SM00481A
116. Ahmadzadegan A, Wang S, Vlachos PP, Ardekani AM (2019) Hydrodynamic attraction of bacteria to gas and liquid interfaces. Phys Rev E 100:062605. https://doi.org/10.1103/PhysRevE.100.062605
117. Desai N, Ardekani AM (2020) Biofilms at interfaces: microbial distribution in floating films. Soft Matter 16:1731. https://doi.org/10.1039/C9SM02038A
118. Hori K, Watanabe H, Ishii S, Tanji Y, Unno H (2008) Monolayer adsorption of a "Bald" mutant of the highly adhesive and hydrophobic bacterium *Acinetobacter* sp. Strain Tol 5 to a hydrocarbon surface. Appl Environ Microbiol 74(8):2511. https://doi.org/10.1128/AEM.02229-07
119. Dasgupta S, Katava M, Faraj M, Auth T, Gompper G (2014) Capillary assembly of microscale ellipsoidal, cuboidal, and spherical particles at interfaces. Langmuir 30(40):11873. https://doi.org/10.1021/la502627h
120. Dewangan NK, Conrad JC (2020) Bacterial motility enhances adhesion to oil droplets. arXiv:2007.13894
121. Binks BP (2002) Particles as surfactants-similarities and differences. Curr Opin Colloid Interface Sci 7(1):21. https://doi.org/10.1016/S1359-0294(02)00008-0
122. Son K, Menolascina F, Stocker R (2016) Speed-dependent chemotactic precision in marine bacteria. Proc Natl Acad Sci 113(31):8624. https://doi.org/10.1073/pnas.1602307113
123. Wang X, Lanning LM, Ford RM (2016) Enhanced retention of chemotactic bacteria in a pore network with residual NAPL contamination. Environ Sci Technol 50(1):165. https://doi.org/10.1021/acs.est.5b03872
124. Haiko J, Westerlund-Wikström B (2013) The role of the bacterial flagellum in adhesion and virulence. Biology 2:1242. https://doi.org/10.3390/biology2041242
125. Friedlander RS, Vogel N, Aizenberg J (2015) Role of flagella in adhesion of *Escherichia coli* to abiotic surfaces. Langmuir 31(22):6137. https://doi.org/10.1021/acs.langmuir.5b00815
126. Das T, Sharma PK, Busscher HJ, van der Mei HC, Krom BP (2010) Role of extracellular DNA in initial bacterial adhesion and surface aggregation. Appl Environ Microbiol 76(10):3405. https://doi.org/10.1128/AEM.03119-09
127. O'Toole GA, Wong GC (2016) Sensational biofilms: surface sensing in bacteria. Curr Opin Microbiol 30:139. https://doi.org/10.1016/j.mib.2016.02.004
128. Müller S, Nebe-von Caron G (2010) Functional single-cell analyses: flow cytometry and cell sorting of microbial populations and communities. FEMS Microbiol Rev 34(4):554. https://doi.org/10.1111/j.1574-6976.2010.00214.x
129. Geng J, Henry N (2011) Short time-scale bacterial adhesion dynamics. In: Linke D, Goldman A (eds) Bacterial adhesion. Advances in experimental medicine and biology, vol 715. Springer, Dordrecht. https://doi.org/10.1007/978-94-007-0940-9_20
130. Ambriz-Aviña V, Contreas-Garduño JA, Pedraza-Reyes M (2014) Applications of flow cytometry to characterize bacterial

physiological responses. BioMed Res Int 2014:461941. https://doi.org/10.1155/2014/461941
131. Kalyuzhnaya M, Lidstrom M, Chistoserdova L (2008) Real-time detection of actively metabolizing microbes by redox sensing as applied to methylotroph populations in Lake Washington. ISME J 2:696. https://doi.org/10.1038/ismej.2008.32
132. Conrad JC, Poling-Skutvik R (2018) Confined flow: consequences and implications for bacteria and biofilms. Annual review of chemical and biomolecular engineering 9:175. https://doi.org/10.1146/annurev-chembioeng-060817-084006